

An Electrochemical Enzymatic Biosensor Based on Au/FGs/sol-gel-GOx Composite/Nafion

Mohammad Faruk Hossain¹, Min Heo², Jae Ho Shin², and Jae Yeong Park^{1,*}

¹ Micro/Nano Devices & Packaging Lab., Department of Electronic Engineering, Kwangwoon University, 447-1, Wolgye-Dong, Nowon Gu, Seoul, 139-701, Korea

² Chemical Sensor Research Group, Department of Chemistry, Kwangwoon University, 447-1, Wolgye-Dong, Nowon Gu, Seoul, 139-701, Korea

*E-mail: jaepark@kw.ac.kr

Received: 9 February 2015 / Accepted: 24 April 2015 / Published: 24 June 2015

We have reported an electrochemical glucose biosensor based on the sol-gel derived composites with glucose oxidase (GOx) and nafion on chemically functionalized graphene sheets (FGs). FGs was developed by chemically treatment of exfoliate graphite oxide and heat treatment of FGs film on the substrate electrode. The as-prepared FGs modified gold thin film electrode exhibited good electrocatalytic behaviors toward oxidation of hydrogen peroxide. Furthermore, the immobilization of GOx was conducted by the entrapment of glucose oxidase in silica-gel network, which became polymerized in the presence of enzyme and nafion is coated on the modified surface. The as-prepared glucose sensor exhibited good performance towards the oxidation of glucose, along with low applied potential, long linear detection range, low detection limit and long period stability, which were assigned to the high active surface area of FGs and allow the entrapment of GOx.

Keywords: Chemically functionalized graphene sheets, Biosensor, Hydrogen peroxide, Glucose, Sol-gel.

1. INTRODUCTION

The fast and efficient determination of glucose has paid attention in the different areas, including the food industry, biotechnology, clinical diagnostics and physiological research [1-4]. In particular, the diagnosis and management of diabetes requires a precise and proper monitoring of the blood glucose level. Diabetes is a worldwide public health problem, resulting from insulin lacking and hyperglycemia, which could be appeared by blood glucose levels higher than the normal range of 4.4-6.6 mM [2]. Especially, amperometric glucose biosensors with simplicity, low cost, and high reliability, based on glucose oxidase (GOx), are extensively used for the detection of the blood glucose

concentration [5-7]. The development of an enzyme based biosensor is a significant factor for the immobilization of enzyme on the sensor surface. Multiple immobilization techniques, such as chemical immobilization in an inert matrix, physical entrapment, and covalent attachment to electrode surfaces have been used to load the relevant enzyme for the construction of the amperometric biosensors [8-10]. Among the various modification procedures, the sol-gel process has attracted much attention for immobilization of biomolecules in the design of the biosensor because of its distinct advantages. Benefit of sol-gel immobilization is that the porous formation of sol-gel matrix simplifies the diffusion of substrates into the matrix and provides capacity for the interaction between substrates and enzymes [11]. In addition, sol-gel techniques can be prepared under low temperature conditions, exhibit chemical inertness, tunable porosity, negligible swelling, optical transparency, low-temperature encapsulation, thermal stability, and biocompatibility [12-14]. To enhance the selectivity and stability of biosensors, nafion is the most desirable one due to its easy handling and commercial availability. It possesses a good surface adhesion to electrode surface and a weak swelling capability in aqueous media.

Graphene is the lattermost form of carbon to be discovered and is the present excited thing in the field of material science. It is a one-atom thick 2D sheet of bonded carbon atoms that are densely packed in a honeycomb crystal lattice and can be observed as an atomic-scale chicken wire made of carbon atoms and their bonds. However, it has attracted remarkable attention, because of its wonderful electrical properties, and the high active surface area of $400 \text{ m}^2 \text{ g}^{-1}$ up to $1500 \text{ m}^2 \text{ g}^{-1}$ for metal nanoparticles (NPs) loading or enzyme adsorption on electrodes. Hence various immobilizing matrices, especially nano materials, including graphene have been used to enhance the electron transfer through substrate electrode [15-17]. The immobilization of the target enzyme loading increases on the surface due to the high surface area of the graphene. The high conductivity and small band gap are conducive for conducting electrons from the biomolecules [18]. Recently, graphene has been used to develop pH sensor, optoelectronic devices, supercapacitors, pH sensor, chemical sensor, and biosensor applications [19-23]. We also prepared a chemically functionalized graphene (FG) based enzymatic glucose biosensor, which presented potential application in biosensors. Particularly, hydrazine, hydrazine hydrate are broadly used reducing agents for chemically converted graphene or chemically functionalized graphene, however these reducing agent are toxic and made to high sheet resistance of FG due to the nitrogen impurities incorporated during reduction process [24]. Another practical way, sodium borohydride is used to reduce FG in aqueous solution. Hydrazine is less effective than sodium borohydride as a reductant of graphite oxide. Sodium borohydride can decrease the sheet resistance of FG [25]. But problem is that, it can be slowly reacted with water. In this context, a little amount of water and more ethylene glycol are beneficial during reduction reactation. Moreover, ethylene glycol acts as a reducing agent of selective functional group and makes the graphite oxide (GRO) extensive dispersion in solution [26].

In this work, chemically functionalized graphene (FG) is developed by wet chemical technique and exfoliated FG is casted Au thin film electrode. Thermal treatment is conducted on FG modified electrode under vacuum oven for getting good performances. The as-prepared electrode is evaluated by measuring particularly electro-catalytic activities towards H_2O_2 . Furthermore, sol-gel derived glucose

oxidase composites with nafion is then immobilized on the FGs modified Au surface and is characterized and analyzed for glucose sensor applications by using electrochemical techniques.

2. EXPERIMENTAL

2.1 Chemicals and apparatus

Methyltrimethoxysilane (MTMOS), ethanol, graphite powder (GRO) (44 μm size), uric acid (UA), acetaminophen (AP), ascorbic acid (AA), hydrogen peroxide (30%), nafion (5%) and β -D(+) glucose were purchased from Aldrich Co. (St. Louis, USA). Chemicals used in experiment were analytical grade. H_2O_2 was mixed in a 0.05 M phosphate buffer (pH 7.4) (PB) solution and all solutions were prepared with ultrapure water (resistivity $\geq 18\text{M}\Omega\text{-cm}$). Human blood plasma was used for testing the biosensor in the biofluidic environmental condition. The developed electrodes were characterized electrochemically by using an electrochemical analyzer of three electrodes systems (Model 600D series, CH Instruments Inc., USA). An Ag/AgCl electrode with 3 mM NaCl and a flat Pt bar were used as reference electrode (RE) and counter electrode (CE), respectively. EIS (Electrochemical impedance spectroscopy) was conducted with the identical electrochemical analyzer and three-electrode configuration in a supporting electrolyte solution of containing 5 mM $[\text{Fe}(\text{CN})_6]^{4-/3-}$ in a frequency range from 0.1 Hz to 100 kHz. The physical characteristics of a developed electrode, GRO and FG were performed by Raman spectroscopy (Raman Nicolet Almega XR Spectrometer), high resolution X-ray photoelectron spectroscopy (XPS; ULVAC-PHI PHI-5000), field emission scanning electron microscopy (FESEM; Hitachi S-4300), and Atomic force microscope (Veeco Metrology Group, NY, USA).

2.2 Synthesis of graphite oxide (GRO) and chemically functionalized graphene (FG)

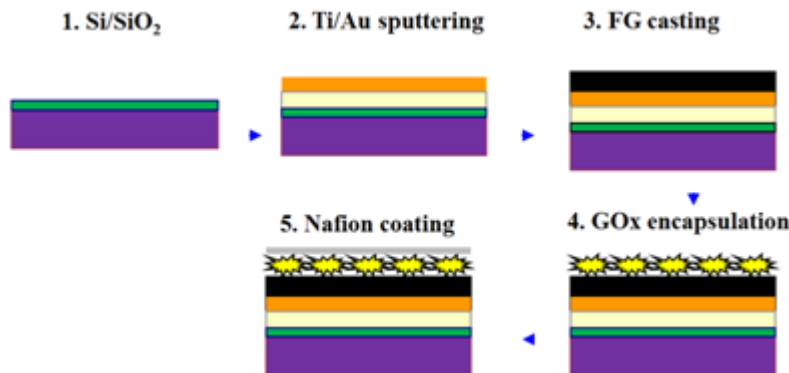
GRO was synthesized by the modified Hummer method [27]. Shortly, 1.5 g of NaNO_3 and 2 g of graphite powder were added into 150 mL of 98% H_2SO_4 solution in a flask immersed in an ice bath. Next, 9 g of KMnO_4 were added a little by little, to the mixture to prevent an unexpected accumulation of heat that is evolved. Afterwards the solution was stirred for 6 days at room temperature. Then, 10 mL of 30% H_2O_2 were dropped into the mixture solution in order to completely react with the remaining KMnO_4 , carrying out a bright yellow solution. To purify the GRO, the resulting mixture was cleaned by 3% H_2SO_4 and H_2O_2 several times until the aqueous solution was reached approximately pH 5–6. The suspension was dried under oven for getting RGO platelets. After that, 40 mL of ethylene glycol were taken into a beaker and mixed 50 mg of GRO platelets. The mixture was followed sonication for 1.5 hours. After that, 30 mL of ultrapure water were dropped into given solution and followed stirring for 1 hour. With the stirring condition, 274 mg of NaBH_4 were added slowly and the mixing solution was heated at 110 $^\circ\text{C}$ for 2 hours. Finally, the mixing solution was filtered and washed several times with ultrapure water and then dried in vacuum oven at 100 $^\circ\text{C}$ at overnight.

2.3 Preparation of Au/FGs

Ti layer of 30 nm of film was sputtered on Si/SiO₂ substrate electrode. Then, a gold layer of 200 nm was sputtered on top of the Ti thin layer. The thin gold was conducted as a seed layer of biosensor electrode. 20 mg of chemically modified graphene powder were dispersed in 20 mL of DMF and ultrapure water solution (1:1). Thereafter, this mixture was ultrasonicated with 180 W for 3.5 hours. Next, 15 μ L of the developed chemically functionalized graphene suspension was cast on the gold thin film plain surface, and dried at ambient environment. After drying, chemically functionalized graphene sheets (FGs) modified thin film Au electrode was rinsed with phosphate buffered (PB) solution and ultrapure water due to remove the loosely attached FGs on the electrode surface, and dried by N₂ gas. Further, the thin film electrode was then put into a vacuum oven at 150 °C during 10 hours to remove oxygen functional groups, moisture, as well as getting good adhesion on the thin film gold surface.

2.4 Preparation of Au/CGs /sol-gel-GOx composites film/nafion

Glucose oxidase (GOx) was prepared according to the succeeding method. 1.6 mg of GOx was dispersed into 200 μ L of ultrapure water. 120 μ L of MTMOS were added into 240 μ L of ethanol and shaken a few time.



Scheme 1. shows the glucose biosensor fabrication procedures.

After that 200 μ L of the GOx solution were mixed with as-prepared ethanol-MTMOS gel, afterwards 20 μ L of HCl (0.1 M) were dropped into as prepared sol-gel composites and stirred for 2 hours. Before dropping the enzyme composites, N₂ plasma was applied onto the FGs surface for 30 s to improve the hydrophilicity of FGs surface. Then, 10 μ L of the as prepared sol-gel composites were dropped onto the surface of FGs modified electrode. Finally, the solvent evaporation was allowed to dry at 4 °C in a refrigerator. Au/sol-gel-GOx was prepared in the same way. Nafion, ethanol and water were mixed with 1:8:1 ratio. 5 μ L of as-prepared nafion was coated on the enzyme modified surface. Both biosensors were stored at 4 °C in a refrigerator when they are not in use. The fabrication procedures of FGs/Sol-gel- GOx/nafion modified electrode are shown in scheme 1.

3. RESULTS AND DISCUSSION

3.1 Morphological characterization of FG

The surface morphology of developed FGs was conducted by FESEM as shown in Fig. 1. The FESEM image of FGs is shown in Fig. 1a, which was made by 3.5 h ultrasonication. A few layers of FG sheets are observed on Au thin film. It also clearly shows a typical wrinkle of FGs made from chemical reduction. The crumpling shape not only reduced the surface energy but also induces mechanical integrity with high tensile strength, Young's modulus, and good film-forming ability due to nano-scale sheets interlocking [28]. Moreover, the oxygen functional groups reduction was assumed to lead the visible crinkle and fold of functionalized graphene, therefore acted good film forming ability with wider surface coverage on the electrode, favorable for mass production of FGs [29-30].

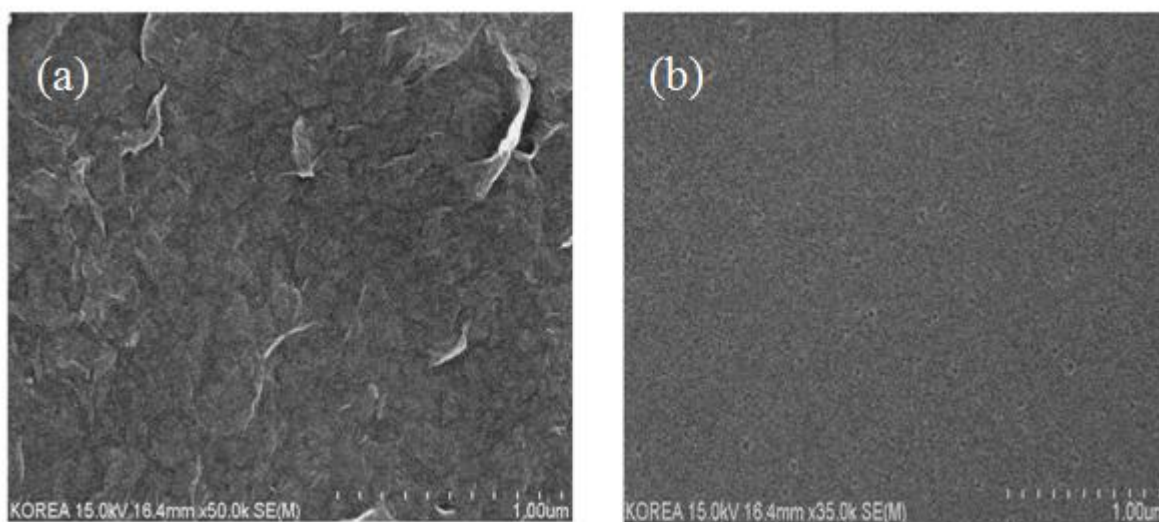


Figure 1. FESEM images of (a) Au/FGs and (b) Au/FGs/GOx-sol-gel composites modified electrode.

When GOx-Sol-gel composite was dropped on the surface of FGs, a porous structure was found on sol-gel film as shown in Fig. 1b. The benefit of porous structure is that molecules easily diffuse on the biosensor surface. Nafion was used for the hindrance of glucose oxidase leakage on the biosensor surface as well as anti-fouling ability against interference species (not given the figure).

Fig. 2a and 2b show C1s XPS spectra of GRO powder and FG sheets respectively. It clearly shows a considerable degree of oxidation that corresponds to carbon atoms in different functional groups. The non-oxygenated ring C (284.6 eV) that involves C=C bond make sp^2 hybridized, C in C=O bonds (288.4 eV) that involves carbonyl groups, and C in C-O bonds (286.2 eV) that includes hydroxyl and epoxy groups [17, 31]. A new peak (285.6 eV) is observed after the reduction of GRO, which is sp^3 hybridized and involves C-C bond [32]. The oxygen functional groups of FGs were much reduced during the chemical reduction reaction, which indicated from the sp^3 hybridized peak.

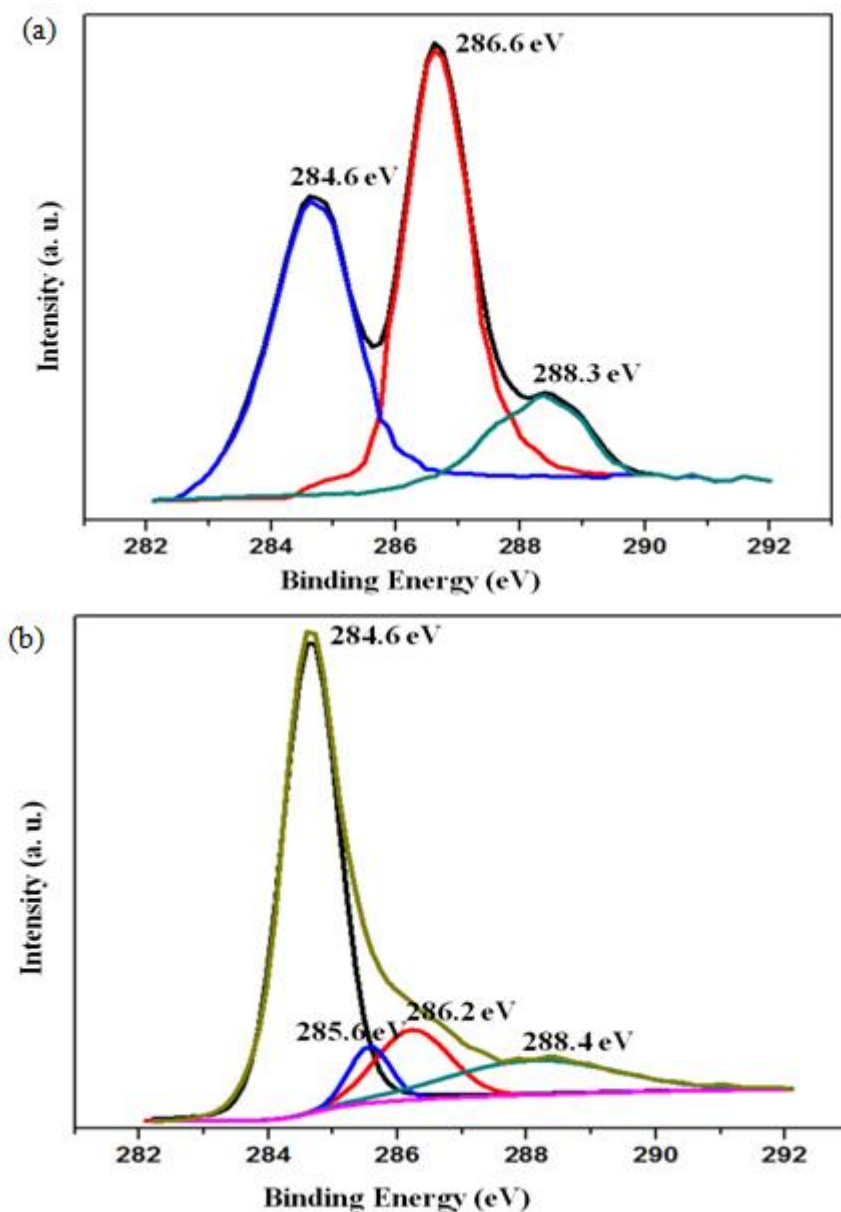


Figure 2. XPS spectra of (a) graphite oxide and (b) FGs.

Fig. 3a shows the Raman spectrum of GRO and chemically functionalized graphene. Generally, the Raman spectra of the materials ensure the observations of the XPS spectrum i.e., the changes of functional groups during the reduction action from GRO to FG. The D peak of FG located at around 1350 cm^{-1} and at 1351 cm^{-1} for GRO streams from a defect-induced breathing mode of sp^2 rings [33]. It is normal to all sp^2 carbon lattices and appears from the stretching of C-C bond. The G peak at around 1590 cm^{-1} for FG and at 1591 cm^{-1} for GRO is due to the first order scattering of the E_{2g} phonon of sp^2 C atoms [33]. The intensity ratio (I_D/I_G) of D band and G band of GRO is about 0.96 while the I_D/I_G of FG is 1.24 due to the existence of unrepaired defects that continued to exist after the removal of large amounts of oxygen-containing functional groups. This I_D/I_G ratio value is similar to the most chemical reduction reports by elsewhere [34].

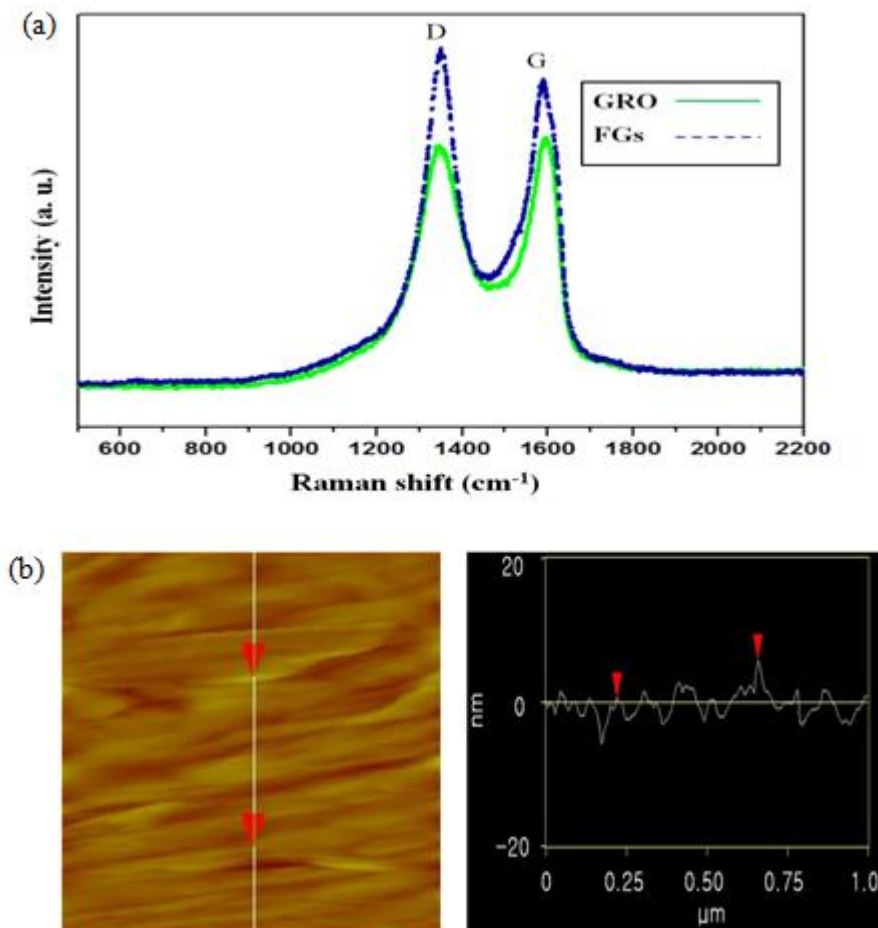


Figure 3. Raman spectra of (a) GRO platelets (solid line) and FG platelets (dotted line), and (b) AFM images of CGs surface (profiles respect to lines chosen in images). Image size $1\ \mu\text{m} \times 0.8\ \mu\text{m}$.

The AFM scan images FGs are displayed in Fig. 3 (b). The surface of FG is slightly rough and this roughness could be due to the presence of functional groups. The estimated thickness is 1-4 nm in the cross sectional view across the plain area of the sheet, which is reported previously [35]. This thickness of FGs indicates that FG consists of mono layer and bi-layer sheets.

3.2 EIS (Electrochemical impedance spectroscopy) of modified electrodes

EIS (electrochemical impedance spectroscopy) was used to characterize the electronic transfer phenomena of the different modified electrodes. Especially, EIS spectra take on two portions i.e. linear line relatively at lower frequencies range correlated with the diffusion process and semicircle at higher frequencies range correlated with the electron transfer limited process. The EIS spectra of the thin plain gold electrode and modified plain electrodes recorded in 0.05 M PB solution containing 5 mM $[\text{Fe}(\text{CN})_6]^{3-/4-}$ fitted with the Randles equivalence circuit model as shown in Fig. 4. There are no well-defined semicircles of bare plain gold electrode and FGs modified Au electrode in the desired frequency range (Fig. 4). This result reveals that indicated electrode possess good electron transfer

kinetics. But when glucose oxidase immobilized with sol-gel composite and nafion on the surface of FGs modified Au electrode, a wider semicircle was existed. Since nafion and sol-gel composite of entrapped GOx was made from polymer, electron transfer resistance of modified electrode should be increased.

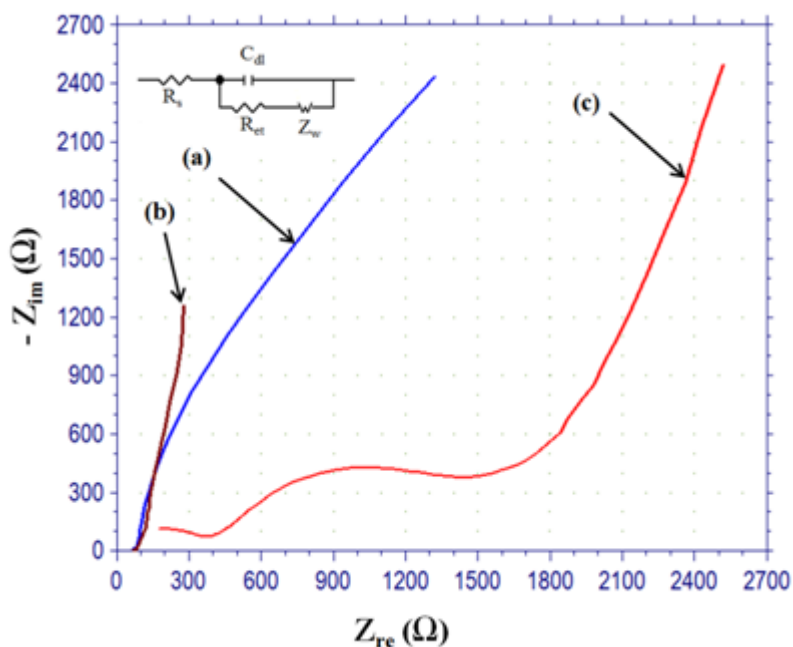


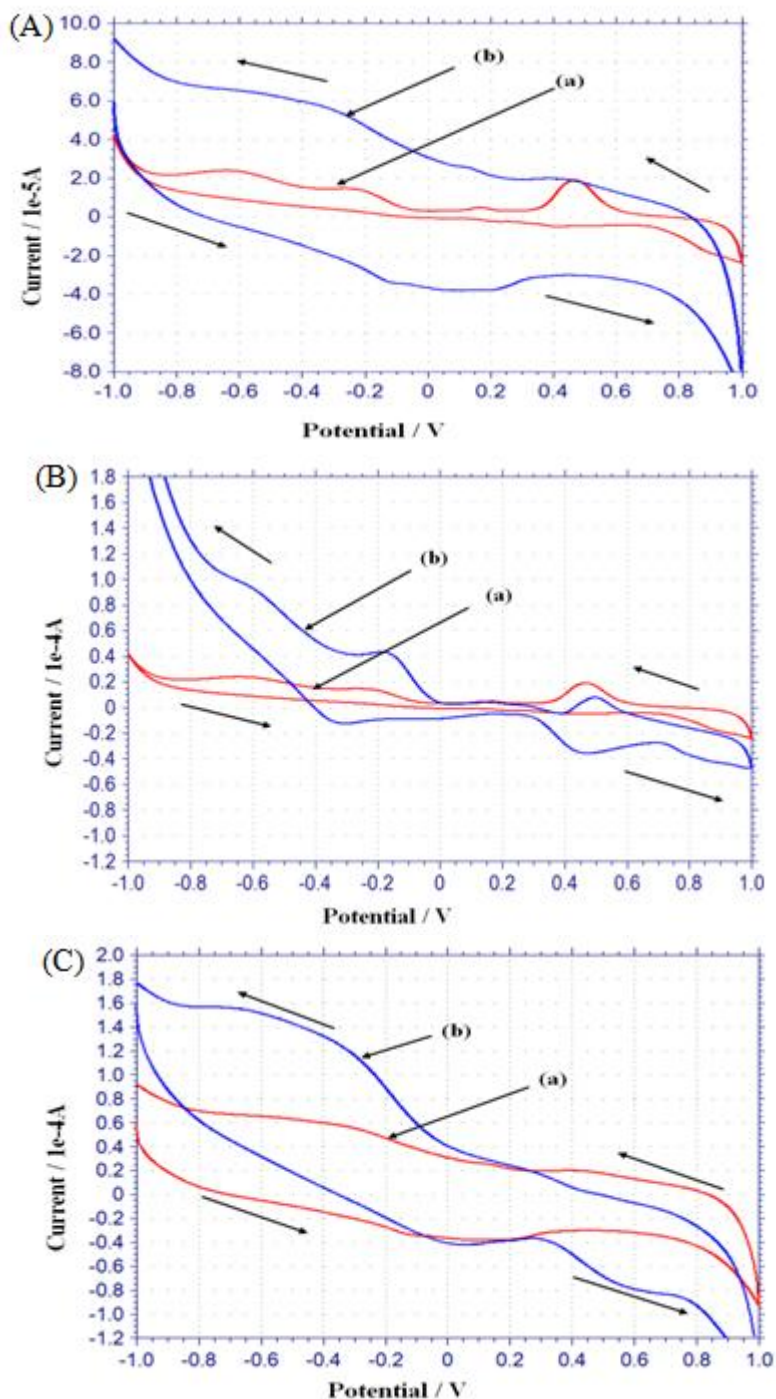
Figure 4. Electrochemical impedance of (a) Plain thin Au, (b) Au/FGs, (c) Au/FGs/sol-gel-GOx/nafion electrode recorded in 0.05 M PB (pH 7.4) with 5 mM $\text{Fe}(\text{CN})_6^{3-/4-}$ solution. Amplitude: 5 mV, frequency: 0.1 Hz to 100 kHz. Randles equivalence circuit utilized to fit the EIS data obtained at all the developed electrodes (inset).

The electron transfer resistance (R_{et}) of plain gold electrode was greater than that of FGs modified plain gold electrode in Fig. 4 (a and b). This result implies that the layer of FGs could form on the electrode surface, and improve the electron transfer from the redox probe of $[\text{Fe}(\text{CN})_6]^{3-/4-}$, to the electrode surface. For nafion with sol-gel derived GOx modified FGs on Au (Fig. 4c), the R_{et} value increased much more, which was approximately 1500 Ω . It is revealed that a high resistance of the electron transfer of the oxidation-reduction pair was created after immobilized of the sol-gel executed GOx composites and nafion on the Au/FGs electrode surface.

3.3 Electrochemical performance of Au/FGs towards H_2O_2

The cyclic voltammograms (CV) of a typical FGs-modified electrode in 0.05 M PB solution are showed in Fig. 5A. The FGs-decorated Au electrode conducted higher background current than plain bare Au electrode in Fig. 5A (a) and (b). The notable background current is due to the catalytically active surface of the modified electrode. After modification of electrode with FGs, the surface area of the electrode increases [36]. In addition, electron transfer rate (electron conductivity) also increases.

Accordingly, the background current at the FGs derived electrode surface is greater than that at the bare plain electrode surface. This characteristic reveals that a good electron transfer exists between the FG sheets and the plain Au electrode [37, 38]. Fig. 5A (a) shows that anodic peak does not appear in the respective potential windows, but three cathodic peaks lie at around 0.47 V, -0.2 V, and -0.6 V.



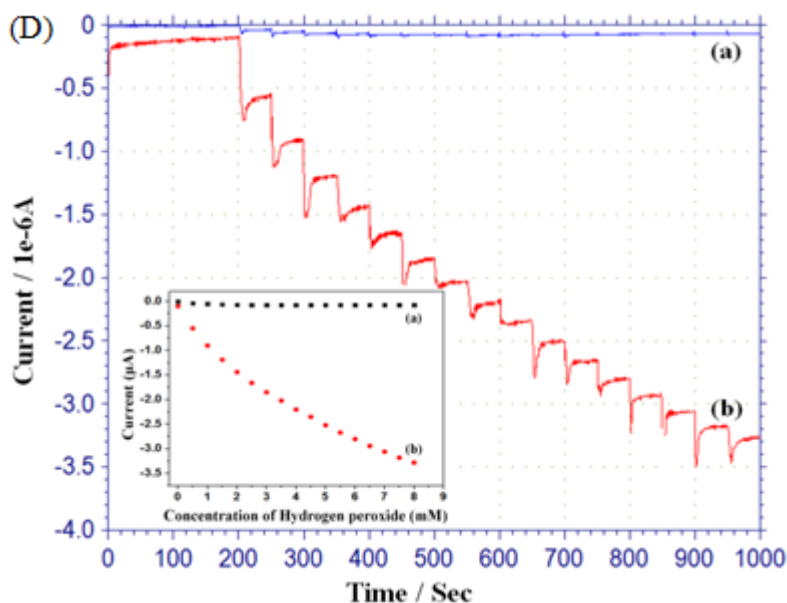


Figure 5. A: Cyclic Voltammograms (CVs) of different developed electrodes (a) bare plain Au, (b) Au/FGs electrodes in 0.05 M PB solution (pH 7.4), scan rate: 50 mV/s. B: CVs of bare Au electrode in (a) PB solution and (b) 2 mM H_2O_2 solution. C: CVs of Au/FGs electrode in PB (a) and in 2 mM H_2O_2 (b). D: Amperometric response of plain bare Au (a) and of Au/FGs (b) electrodes in 0.05 M PB solution to the consecutive addition of 0.5 mM H_2O_2 solution at 0.3 V (with inset calibration curve).

The peak exists at 0.47 V in cathodic direction, which indicates the reduction of single layer gold oxide. Another peak at around -0.2 V is due to reduction of recalcitrant metal oxide, which may appear during anodic sweep. The peak at -0.6 V involves in the hydrogen desorption on gold nanostructured surface. In Fig. 5A (b), a broad anodic peak (-0.2 V to 0.25 V) and a broad cathodic peak (0.0 V to -0.6) are observed. The cathodic peak and the anodic peak are assigned to the redox couple of some electrochemically active oxygen-functional groups in FG sheets that are too steady to be reduced by the chemically and thermally [39].

The CVs of a typical bare Au thin film electrode in 0.05 M PB solution and PB solution with 2 mM H_2O_2 solution are presented in Fig. 5B. From Fig 5B, it is clear that bare Au electrode is electrochemical active towards redox reaction of H_2O_2 . There is no oxidation peak in only PB solution but, one oxidation peak observes due to oxidation of H_2O_2 in H_2O_2 concentrated solution. It is also seen that the reduction peak of bare Au electrode at 0.5 V in 2 mM H_2O_2 concentrated solution is smaller than that of bare Au electrode in only PB solution. This result indicates that poison intermediates adsorption on the surface that reduces the electron conductivity of Au electrode. But after 0.0 V, current response of Au electrode in 2 mM H_2O_2 concentrated solution is higher than that of Au electrode in only PB solution. This may be occurred due to high reduction reaction of H_2O_2 at that potentials region. The CVs of as-prepared Au/FGs electrode in 0.05 M PB solution and PB with 2 mM H_2O_2 solution are presented in Fig. 5C. From Fig. 5C (b), it is seen that a new oxidation peak arises after injection of H_2O_2 due to the oxidation of H_2O_2 . After injection of H_2O_2 , catalytic performance of Au/FGs has increased abruptly. Au/FGs display much more favorable electrochemical activities

towards the catalysis of H_2O_2 than does the bare Au electrode in terms of current response (Figs. 5B and 5C). It is worth noting that cyclic voltammograms of different modified electrodes are presented separately due to clearly visible of the peaks.

The current response increases rapidly from applied potential at 0.3 V during oxidation of H_2O_2 that are observed in Figs. 5B and 5C. Besides, oxidation peak of glucose is observed at that potential, which is described subsequent section. Therefore, the operational potential of 0.3 V was selected for oxidation of H_2O_2 in the following experiments. Current responses are an important factor for evaluation of an amperometric sensor. Therefore, the current responses were observed under different concentrations of H_2O_2 at a given potential as shown in Fig. 5D. The amperometric response of thin film Au electrode is shown in Fig. 5D (a) at +0.3 V upon consecutive droppings of H_2O_2 in PB solution, and calibration curves are shown in the inset of the figure. In this figure, it is seen that with the addition of H_2O_2 to the PB solution, the current response is negligible as compared to the current response of Au/FGs electrode. This consequence indicates that interim poison affects the catalytic surface and interrupts the current through the electrode. Fig. 5D (b) exhibits the amperometric response of Au/FGs at +0.3 V upon consecutive droppings of H_2O_2 to the PB solution and respective calibration curve in the inset of figure. The sensitivity of the sensor is $2.05 \mu\text{A}/\text{mMcm}^2$ at +0.3 V, with linear detection range of 0.5 - 8 mM, and response time of 3 seconds. From Figs. 5D (a) and (b), the amperometric response of FGs modified electrode is higher than that of bare plain Au electrode. This consequence reveals that FGs modified electrode exhibits strong electrocatalytic activity towards oxidation of H_2O_2 at that potential.

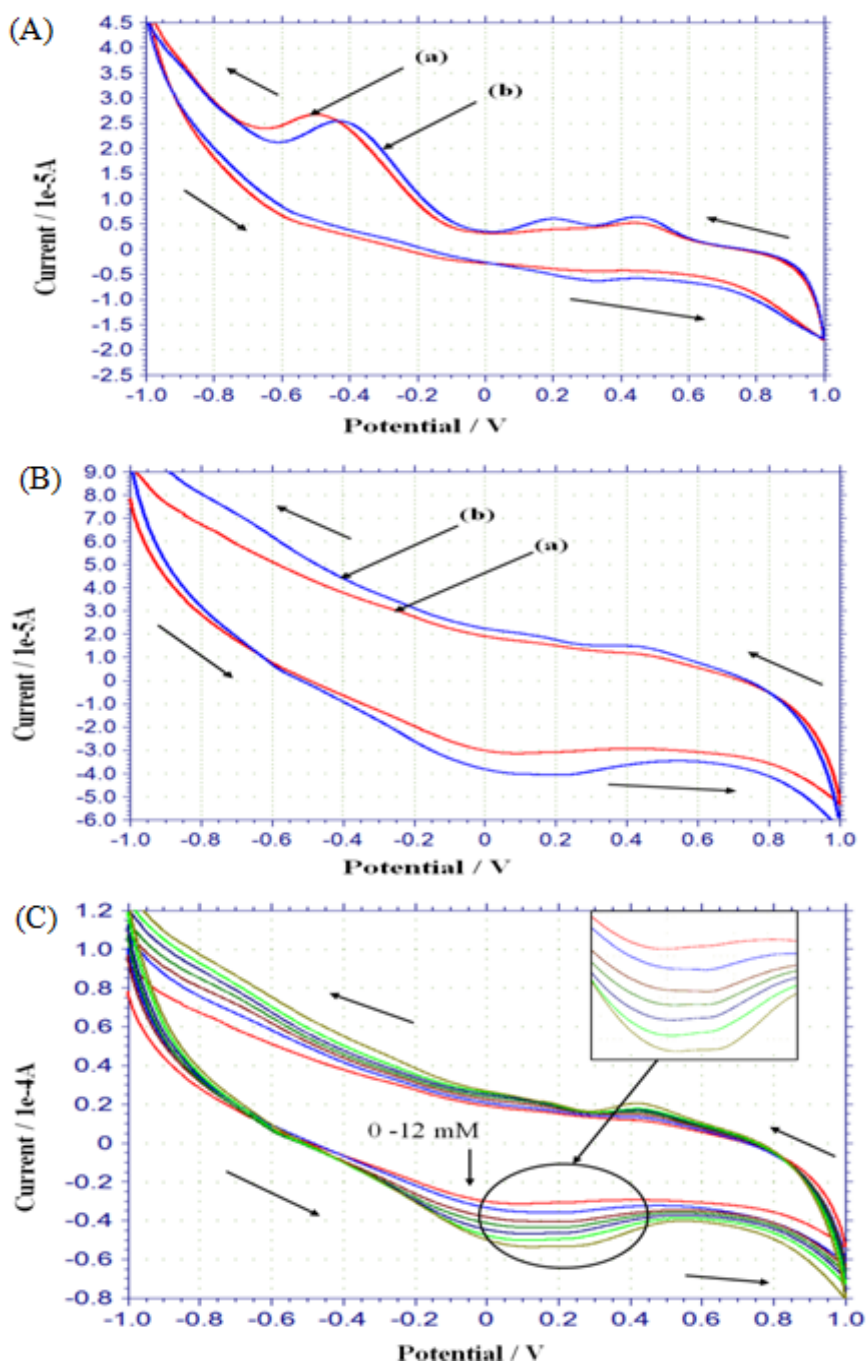
3.4 Electrocatalytic implementation of Au/FGs/sol-gel-GOx/nafion for glucose sensing

The CVs of a typical enzyme decorated electrodes in 0.05 M PB solution and PB with 4 mM glucose solution are presented in Fig. 6A. After deposition of glucose oxidase on the surface of bare plain gold electrode, the intensity of oxidation and reduction peaks has been abated. This result indicates that a barrier layer may be formed against electron movement.

In Fig. 6A (a), it is seen that there is no oxidation peak but two reduction peaks present on the cathodic sweep. There is a weak cathodic peak at 0.45 V, which can be undergone due to reduction of gold oxide. But the peak at -0.5 V may attribute due to the adsorbed GOx catalyzed the reduction of dissolved oxygen and resulted in a massive enhancement in the reduction peak current [40]. In Fig. 6A (b), it shows the CV of Au/ sol-gel-GOx/nafion in PB with 4 mM glucose solution. It is seen that there is an anodic peak and three cathodic peaks due to present of glucose.

An anodic peak arises owing to the oxidation of glucose and a new cathodic peak forms due to the adsorption of poison intermediate. It is also seen that cathodic peak at -0.42 V has reduced more than without glucose, which ascribes the reduction of oxygen from solution. The CVs of a typical Au/FGs/ sol-gel-GOx/nafion electrode in 0.05 M PB solution and PB with 4 mM glucose solution are presented in Fig. 6B. In Fig. 6B (a), there is no obvious anodic and cathodic peak due to the barrier layer produced for loading of GOx on the FGs modified electrode. After injection of 4 mM glucose in the PB solution, an anodic and a cathodic peak are observed on positive and negative sweep as shown

in Fig. 6B (b). This redox peak is the contribution of the redox reaction of the FAD of glucose oxidase. From this figure, it is also clear that anodic peak current is higher than that of cathodic peak current because of lower dissolve oxygen in solution. This result is good agreement with other similar reports [41-42]. Fig. 6C shows the cyclic voltammograms obtained with the Au/FGs/sol-gel-GOx/nafion biosensor electrode in 0.05 M PB solution with the addition of glucose. A broad oxidation peak is observed from 0.0 V to 0.4 V. Moreover, the current decreased linearly (inset of Fig. 6C) against the concentrations of glucose ranging from 2 mM to 12 mM. Sensitivity of the biosensor was found to 9.14 $\mu\text{A}/\text{mMcm}^2$ at 0.3V.



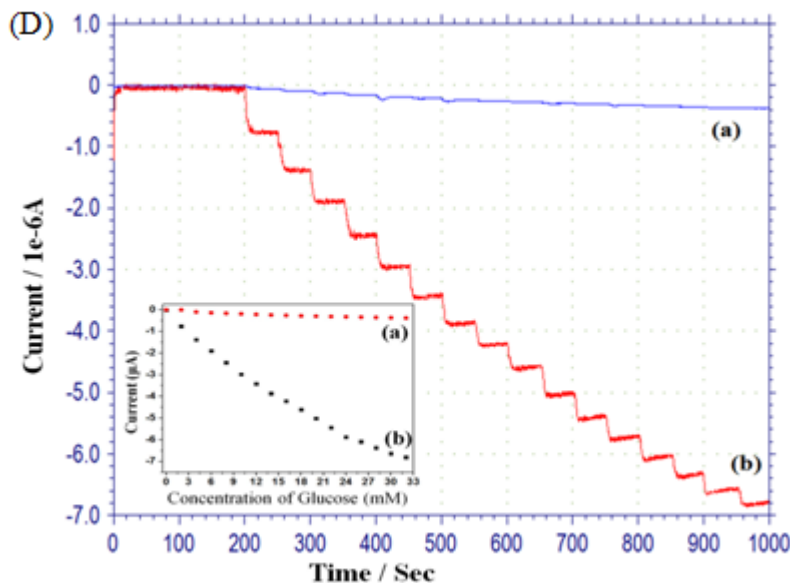


Figure 6. A: Cyclic Voltammograms (CVs) of as-prepared Au/sol-gel-GOx/nafion electrode in 0.05 M PB solution (a) and in 4 mM glucose (b). B: CVs of as- prepared Au/FGs/sol-gel-GOx/nafion electrode in PB (pH 7.4) (a) and in 4 mM glucose (b). C: CVs of Au/FGs/sol-gel-GOx/nafion in PB solution in different concentration of glucose (0-12 mM). D: Amperometric response of Au/sol-gel-GOx/nafion (a) and of Au/FGs/sol-gel-GOx/Nafion (b) electrodes in 0.05 M PB solution to the consecutive additions of glucose in 2 mM at 0.3 V, (inset calibration curve).

For optimization, the amperometric current was measured at 0.3 V because it was seen that hydrogen peroxide was oxidized more at this peak potential. Fig. 6D (a) exhibits the amperometric assessment of Au/sol-gel-GOx/nafion at 0.3 V upon consecutive injections of glucose (2 mM) in PB solution, and the corresponding calibration curve is observed in the inset of this figure. Current response of GOx modified electrode is very low.

Table 1. Comparison of several glucose biosensor electrodes

Sample	Detection range	Sensitivity	References
GCE/AuNP-GOx-Nafion	0.2-20 mM	0.4 $\mu\text{A}/\text{mMcm}^2$	[43]
Pt/GOx-sol-gel	2-18 mM	0.1067 $\mu\text{A}/\text{mM}$	[44]
PNR/sol-gel-GOx/PU	0.05-0.5 mM	0.117 $\mu\text{A}/\text{mM}$	[45]
GCE/PLL/ERGO/GOx	0.25-5 mM	-	[46]
GCE/PVP-RGO/PFIL-GOx	2-14 mM	-	[47]
Au/FGs/sol-gel-GOx/Nafion	2-24 mM	0.24 $\mu\text{A}/\text{mM}$	[This work]

*PFIL- polyethylenimine-functionalized ionic liquid
 PLL- poly l-lysine

Fig. 6D (b) displays the amperometric response of Au/FGs/sol-gel-GOx/nafion glucose biosensor electrode at 0.3 V applied potential upon consecutive droppings of 2 mM glucose in PB solution, and the respective calibration curve is exhibited in the inset of this figure. From this figure, it

is seen that the sensitivity of $1.2 \mu\text{A}/\text{mMcm}^2$ ($R^2=0.993$) with a linear detection range of 2 -24 mM, response time 5 s. The detection limit of glucose was also observed to be $40 \mu\text{M}$. Various glucose sensors are given in the Table 1 with respect to sensitivity and the linear range [43-47]. The performance of the developed biosensor is fairly good in comparison with the indicated glucose biosensors in Table 1.

3.5 Interference effect, stability, reproducibility and blood plasma test on biosensor electrode

The interferences from electroactive compounds commonly confer in physiological samples of glucose such as uric acid (UA), acetaminophen (AP), and ascorbic acid (AA) usually faced problems in the accurate determination of glucose.

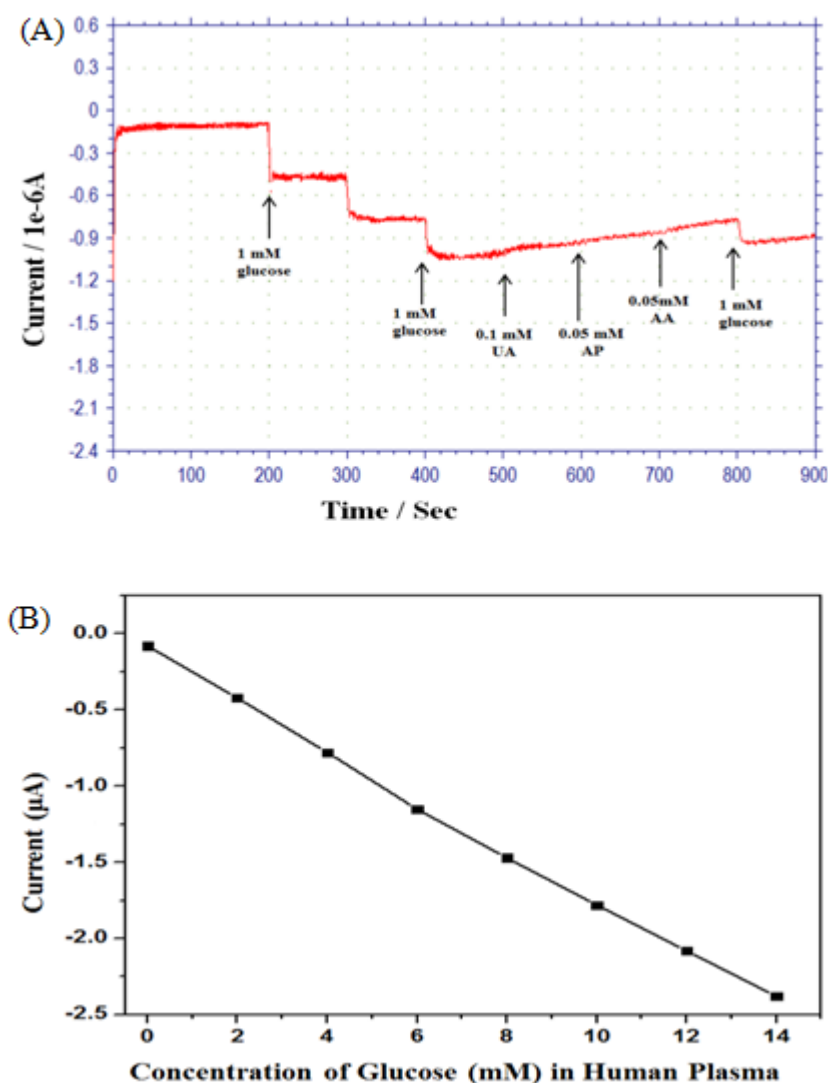


Figure 7. A: Plot diagram of (a) interference effect of different interference species (0.1 mM UA, 0.05 mM AP and 0.05 mM AA) of biosensor electrode in PB solution with 3 mM glucose. B: Amperometric responses of biosensor electrodes in PB solution for consecutive injection of glucose in human blood plasma.

The effects of those possible interfering substances upon the response of the glucose biosensor were evaluated at 0.3 V. Interference effect of biosensor electrode has been seen in Fig. 7A. From this figure, it is clear that there is no significance effect by dropping of 0.1 mM UA, 0.05 mM AP and 0.05 mM AA in the presence of 3 mM glucose on the biosensor electrode.

The stability of the glucose biosensor was performed by means of the amperometric measurements over period of four weeks using 6 mM glucose. It was determined that the glucose sensor response decreased by 20% of its initial response over a period of four weeks. This result reveals that FGs has some functional groups at the edge plane (carboxyl and phenolic groups). Upon dropped GOx composite and nafion onto the surface of FG sheets, the functionalities of graphene sheets at the edge planes can easily bind with the free amine terminals of GOx through covalent linkage [48].

The reproducibility of the biosensor electrode response depends mainly on the reproducibility of the synthesized FGs and GOx composites in the same condition. For reproducibility test, four Au/FGs/sol-gel-GOx/nafion biosensors electrode were developed as the similar process that the particular biosensor was made. Each sensor was measured in consecutive addition of 2 mM to 6 mM glucose in the PB solution. Four different biosensors show standard deviation of 6.5% in amperometric current response. It is concluded that the developed biosensors electrode had an acceptable reproducibility respect to the amperometric measurement.

In order to evaluate the performance of Au/FGs/sol-gel-GOx/nafion biosensor electrode, glucose in human blood plasma solution was detected. The current response with successive injection of 2 mM glucose of blood plasma was measured in PBS solution. The current response of as prepared glucose biosensor is shown in Fig. 7B. It exhibited stable and continuous current response (2-14 mM) at biofluidic solutions. Similar results have also been found as previously reported works [49-50].

4. CONCLUSIONS

Chemically functionalized graphene (FG) was effectively developed by the exfoliation of graphite oxide (GRO), and Au/FGs electrode was fabricated. The developed electrode exhibited a good catalytic activity towards the oxidation of H_2O_2 . It also exhibited good electrochemical properties, with the sensitivity of $2.05 \mu\text{A}/\text{mMcm}^2$ and linear detection range of 0.5-8 mM and a short response time of 3 s towards H_2O_2 oxidation. Upon dropped the GOx- sol-gel composites with nafion on the surface of the Au/FGs electrode, GOx made covalent bond with functional groups of FGs. This as-prepared biosensor electrode exhibited high electrocatalytic activity towards the oxidation of glucose in PB solution, with a response time of 5 s, sensitivity of $1.2 \mu\text{A}/\text{mMcm}^2$, and linear detection range of 2-24 mM. It also showed good stability, reproducibility, low interference effect of interference species as well as a long linearity for glucose sensing in human blood plasma.

ACKNOWLEDGEMENT

This research was partially supported by the Industrial strategic technology development program (10041876) funded by the Ministry of Trade, Industry & Energy (MI, Korea) and by research grant of

Kwangwoon University in 2014. The authors are grateful to MiNDaP (Micro/Nano Device & Packaging Lab.) group members at the Department of Electronic Engineering, and Plasma Bioscience Research Center, Kwangwoon University for their technical discussion and support.

References

1. K. J. Cash and H. A. Clark, *Trend in Mole. Medi.*, 16 (2010) 584.
2. J. Wang, *Chem. Rev.*, 108 (2008) 814.
3. E. S. McLamore, J. Shi, D. Jaroch, J. C. Claussen, A. Uchida, Y. Jiang, W. Zhang, S. S. Donkin, M. K. Banks, K. K. Buhman, D. Teegarden, J. L. Rickus and D.M. Porterfield, *Biosens. Bioelectron.*, 26 (2011) 2237.
4. J. Shi, E. S. McLamore, D. Jaroch, J. C. Claussen, J. L. Rickus and D. M. Porterfield, *Anal. Biochem.*, 411 (2011) 185.
5. A. Heller and B. Feldman, *Chem. Rev.*, 108 (2008) 2482.
6. D. Zhai, B. Liu, Y. Shi, L. Pan, Y. Wang, W. Li, R. Zhang, G. Yu, *ACS Nano*, 7 (2013) 3540.
7. T. Kong, Y. Chen, Y. Ye, K. Zhang, Z. Wang and X. Wang, *Sens. Actu. B chem.*, 138 (2009) 344.
8. W. Y. Lee, K. S. Lee, T. H. Kim, M. C. Shin and J. K. Park, *Electroanal.*, 12 (2000) 78.
9. Y. Wang, L. Liu, D. Zhang, S. Xu and M. Li, *Electrocat.*, 1 (2010) 230.
10. F. Wang, J. Yao, M. Russel, H. Chen, K. Chen, Y. Zhou, B. Ceccanti, G. Zaray, M. M. Choi, *Biosens. Bioelectron.*, 25 (2010) 2238.
11. J. Shi and D. Marshall Porterfield, Prof. Pier Andrea Serra (Ed.), ISBN: 978-953-307-328-6, InTech (2011).
12. K. Thenmozhi and S. S. Narayanan, *Sens. Act. B chem.*, 125 (2007) 195.
13. R. E. Sabzi, S. Zare, K. Farhadi and G. Tabrizvand, *J. China Chem. Soc.*, 52 (2005) 1084.
14. G. Fu, X. Yue and Z. Dai, *Biosens. Bioelectron.*, 26 (2011) 3973.
15. J. R. Anusha, H. J. Kim, A. T. Fleming, S. J. Das, K. H. Yu, B. C. Kim and C. J. Raj, *Sens. Act. B Chem.*, 202 (2014) 827.
16. G. Eda, G. Fanchini and M. N. Chhowalla, *Nanotech.*, 3 (2008) 270.
17. R. Manjunatha, D. H. Nagaraju, G. S. Suresh, J. S. Melo, S. F. D'souza and T. V. Venkatesha, *J. Electroanal. Chem.*, 651 (2011) 24.
18. S. Stankovich, D. A. Dikin, G. H. B. Dommett, K. M. Kohlhaas, E. J. Zimney, E. A. Stach, R. D. Piner, S. T. Nguyen and R. S. Ruoff, *Nature*, 442 (2006) 282.
19. Y. Xu, Z. Lin, X. Huang, Y. Liu, Y. Huang and X. Duan, *Am. Chem. Soc.*, 5 (2013) 4042.
20. B. M. Giacchetti, A. Hsu, H. Wang, V. Vinciguerra, F. Pappalardo, L. Occhipinti, E. Guidetti, S. Coffa, J. Kong and T. Palacios, *J. App. Phy.*, 114 (2013) 084505.
21. G. Yang, C. Lee, J. Kim, F. Ren and S. J. Pearton, *Phy. Chem. Chem. Phy.*, 15 (2013) 1798.
22. X. H. Zhou, L. H. Liu, X. Bai and H. C. Shi, *Sens. Act. B chem.*, 181 (2013) 661.
23. D. W. Boukhvalov and M. I. Katsnelson, *J. Ame. Chem. Soc.*, 130 (2008) 10697.
24. J. Zhang, H. Yang, G. Shen, P. Cheng, J. Zhang and S. Guo, *Chem. Commun.* 46 (2010) 1112.
25. H. J. Shin, K. K. Kim, A. Benayad, S. M. Yoon, H. K. Park, I. S. Jung, M. H. Jin, H. K. Jeong, J. M. Kim, J. Y. Choi and Y. H. Lee, *Adv. Func. Mat.*, 19 (2009) 1987.
26. S.W Lee, J. Kim, S. Chen, P.T. Hammond and Y. Shao-Horn, *ACS Nano*, 4 (2010) 3889.
27. W. S. Hummers and R. E. Offeman, *J. Am. Chem. Soc.*, 80 (1958) 1339.
28. J. Yang, S. Deng, J. Lei, H. Ju and S. Gunasekaran, *Biosen. Bioelectron.*, 29 (2011) 159.
29. H. L. Guo, X. F. Wang, Q. Y. Qian, F. B. Wang and X. H. Xia, *J. Am. Chem. Soc.* 3 (2009) 2653
30. R. Kumar, A. K. Sharma, M. Bhatnagar, B. R. Mehta and S. Rath, *Nanotech.* 24 (2013) 165402.
31. S. Woo, J. Lee, S. K. Park, H. Kim, T. D. Chung and Y. Piao, *Current Applied Physics*, 15 (2015) 219.

32. Q. Du, M. Zheng, L. Zhang, Y. Wang, J. Chen, L. Xue, W. Dai, G. Ji and J. Cao, *Electrochim. Acta*, , 55 (2010) 3897.
33. A. C. Ferrari and J. Robertson, *Phys. Rev. B*, 61 (2000) 14095.
34. Z. Fan, K. Wang, T. Wei, J. Yan, L. Song and B. Shao, *Carbon*, 48 (2010) 1670.
35. D. Joung, A. Chunder, L. Zhai and S. I. Khondaker, *Nanotech.*, 21 (2010) 165202.
36. P. Wu, Q. Shao, Y. Hu, J. Jin, Y. Yin, H. Zhang and C. Cai, *Electrochim. Acta*, 55 (2010) 8606.
37. C. Shan, H. Yang, D. Han, Q. Zhang, A. Ivaska and L. Niu, *Biosens. Bioelectron.*, 25, 1070 (2010).
38. H. W. Yang, M. Y. Hua, S. L. Chen and R. Y. Tsai, *Biosens. Bioelectron.*, 41 (2013) 172.
39. D. Chen, Y. Tang, K. Wang, C. Liu and S. Luo, *Electrochem. Comm.*, 13 (2011) 133.
40. S. Liu and H. Ju, *Biosens. and Bioelectron.*, 19 (2003) 177.
41. D. Savitri and C. K. Mitra, *Bioelectrochem. Bioenerg.*, 47 (1998) 67.
42. B. Liang, L. Fang, G. Yang, Y. Hu, X. Guo and X. Ye, *Biosens. Bioelectron.*, 43 (2013) 131.
43. S. Thibault, H. Aubriet, C. Arnoult and D. Ruch, *Microchim. Acta*, 163 (2008) 211.
44. N. Demirkiran, E. Ekinci and M. Asilturk, *J. Chil. Chem. Soc.*, 57 (2012) 1336.
45. R. Pauliukaite, M. Schoenleber, P. Vadgama and C. M. A. Brett, *Anal. Bio-anal. Chem.*, 390 (2008) 1121.
46. L. Hua, X. Wu and R. Wang, *Anal.*, 137 (2012) 5716.
47. C. Shan, H. Yang, J. Song, D. Han, A. Ivaska and L. Niu, *Anal. Chem.*, 81 (2009) 2378.
48. S. Alwarappan, C. Liu, A. Kumar and C. Z. Li, *J. Phys. Chem. C*, 114 (2010) 12920.
49. Y. J. Lee, D. J. Park and J. Y. Park, *IEEE SENS. J.*, 8 (2008) 1922.
50. J. Yu, S. Liu and H. Ju, *Biosens. Bioelectron.*, 19 (2003) 401.

© 2015 The Authors. Published by ESG (www.electrochemsci.org). This article is an open access article distributed under the terms and conditions of the Creative Commons Attribution license (<http://creativecommons.org/licenses/by/4.0/>).